Structural, electronic and magnetic properties of Mn-doped GaAs(110) surface

A. Stroppa(*)

Dipartimento di Fisica Teorica, Università di Trieste
Strada Costiera 11, I-34014 Trieste, Italy
INFM DEMOCRITOS National Simulation Center - Trieste, Italy

Summary. — First principles total-energy pseudopotential calculations have been performed to investigate STM images of the (110) cross-sectional surface of Mn-doped GaAs. We have considered configurations with Mn in interstitial positions in the uppermost surface layer with Mn surrounded by As (Int_{As}) or Ga (Int_{Ga}) atoms. The introduction of Mn on the GaAs(110) surface results in a strong local distortion in the underlying crystal lattice, with variations of interatomic distances up to 3% with respect to unrelaxed ones. In both cases, the surface electronic structure is half-metallic (or *nearly* half metallic) and it strongly depends on the local Mn environment. The nearby Mn atoms show an induced spin-polarization resulting in a ferromagnetic Mn–As and antiferromagnetic Mn–Ga configuration. The simulation of the STM images show very different pattern of the imaged Mn atom, suggesting that they could be easily discerned by STM analysis.

PACS 73.20.At – Surface states, band structure, electron density of states.
PACS 75.50.Pp – Magnetic semiconductors.
PACS 75.70.Rf – Surface magnetism.
PACS 71.55.Eq – III-V semiconductors.

1. – Introduction

The easy integration of ferromagnetism with semiconducting properties in the same host material provided by Diluted Magnetic Semiconductors (DMSs) has been considered an important breakthrough in the semiconductor microelectronics. This is mainly due to the unprecedented opportunity to create a new class of devices which would combine the spin degree of freedom to process, to transfer as well as to store information. *Spintronics* is the emergent technology which exploits the quantum propensity of electrons to spin as well as their charge state [1-3].

(*) E-mail: astroppa@ts.infn.it

The discovery of ferromagnetism in Mn-doped GaAs semiconductor has become a milestone in spintronic revolution: $Mn_xGa_{1-x}As$ alloys are directly related to the existing GaAs technology, resulting in the practical realization of device structures combining ferromagnetic and nonmagnetic layers [4].

There are several possibilities for a single Mn to be incorporated in the GaAs. It can occupy either the cation site (substitutional Mn, Mn_{Ga}) or the anion site (As antisite, Mn_{As}); it can also occupy interstitial sites, as reported by Yu *et al.* [5]. Further, other structural defects could be present in the alloy, such as As antisite (As_{Ga}). The fraction of Mn dopants occupying one or another location depends on the growth conditions and techniques [6].

The Curie temperature (T_c) is a key parameter in designing room-temperature spintronic devices. The highest T_c reachable for $Mn_xGa_{1-x}As$ up to few years ago was 110 K [4], *i.e.* rather low for practical technological purposes. It has been shown that interstitial Mn atoms have a crucial role in magnetic properties of the samples [7,8]. An intense experimental and theoretical effort has been pursued in the last years in order to understand the physics of this material and how to raise the Curie temperature.

Nowadays, a new method has been proposed as an alternative to the growth by Molecular Beam Epitaxy (MBE) of bulk $Mn_xGa_{1-x}As$ random alloy: the dopant atoms are incorporated in the sample in such a way to give rise to a Dirac δ-function concentration profile (with locally high dopant concentration) along the grow direction (δ-doping) [9]. Remarkably, an important enhancement of T_c is obtained in these δ-doped samples (the highest T_c obtained so far with δ-doped sample is 250 K) [10]. Very recently, Mn δ-doped GaAs samples in (001) direction have also been grown at TASC Laboratory in Trieste [11].

Therefore clarifying the site geometry and the local environment of impurities in δ-doped GaAs:Mn should shed light on the understanding and the optimization of the magnetic properties of the system. From the experimental point of view, this study can be pursued with cross-sectional Scanning Tunneling Microscopy (XSTM): the Mn-doped GaAs samples are cleaved along the natural (110) cleavage plane and then analyzed by STM microscopy.

In recent years, several XSTM studies on $Mn_xGa_{1-x}As$ alloys have been performed but the local environment (and preferential geometric site) of defects has not been clarified yet [12-15]. From the theoretical point of view, the existing simulated XSTM images have mainly focused on the characterization of substitutional impurities on uppermost surface layers, while a complete and detailed investigation of interstitial impurity on uppermost surface layers is still lacking thus preventing the possibility of a full interpretation of the new XSTM images acquired.

Therefore, stimulated by the recent growth and following XSTM analysis of Mn δ-doped GaAs samples at TASC [11], we have performed density functional calculations to investigate the structural, electronic and magnetic properties of a single Mn dopant, by focusing our attention on the impurity *interstitial* surface configurations. We have also simulated the corresponding STM images.

This paper is organized as follows: in the next section we describe the computational method; in sect. **3** we present our results for the structural, electronic and magnetic properties; in sect. **4** we discuss our results for the XSTM images; finally, in sect. **5** we draw our conclusions.

2. – Computational details

Our study has been performed within Density Functional Theory (DFT) framework in the Local Spin Density Approximation (LSDA) for the exchange-correlation (XC) functional by using state-of-the-art first-principles pseudopotential self-consistent calculations, as implemented in the ESPRESSO/PWscf code [16]. We used the scheme of Ceperley and Adler [17] (with the parametrization of Perdew and Zunger [18]) for XC functional. Mn atom is described by an ultrasoft (US) pseudopotential (PP) [19] while norm-conserving PPs have been considered for Ga, As and H atoms.

Test calculations have shown that a kinetic energy cut-off for the wave functions equal to 22 Ry and a 200 Ry cut-off for the charge density are sufficient to get well-converged results. We estimate the numerical uncertainty to be ~ 0.01 Å for relative atomic displacements and $\sim 0.02 \ \mu_B$ for the magnetic moments. The relaxed internal atomic positions have been obtained by total-energy and atomic-force minimization using the Hellmann-Feynman theorem [20].

The surface is modelled with periodically repeated cell containing one Mn atom; a (110) slab geometry with a 4×4 in-plane periodicity has been used. The simulation cells are made up of 5 atomic layers and a vacuum region equivalent to 8 atomic layers. The bottom layer has been passivated with hydrogen atoms in order to simulate semi-infinite bulk material [21]. In the energy minimization only the three uppermost layers are allowed to relax, while the others are considered bulk-like.

Two different configurations have been considered for Mn on the surface, namely $Int_{As(Ga)}$ with As (Ga) atoms as nearest-neighbor atoms. In each case, the distances between the Mn atom and its periodic image on the (110) plane are 15.7 Å along the $[1\bar{1}0]$ and 22.2 Å along [001].

XSTM images are obtained within Tersoff-Hamann model [22], where the constant current STM images are simulated from electronic structure calculations by considering surfaces of constant integrated local density of states.

3. – Structural, electronic and magnetic properties

3'1. *Structural properties*. – The GaAs(110) surface is well known from an experimental as well as a theoretical point of view [23]. In fig. 1, we show a ball and stick model of the clean surface, side and top views. The surface unit cell in shown in the top view. In this and the other figures, black spheres are cations (Ga atoms), grey spheres are anions (As atoms).

At the top layer, the Ga surface atoms relax inward while the As atoms are shifted above the surface. Due to overbinding in the LDA approximation, our theoretical GaAs lattice constant (5.55 Å) is smaller than the experimental one (5.65 Å) but the relevant calculated structural parameters for the clean surface such as $\Delta_{1,\perp}$ (relative displacement of the anion and cation positions in the uppermost layer, normal to the surface) and α (the buckling angle), shown in fig. 1, are 0.68 Å and 30.36°, respectively, which well compare with the experimental values 0.65±0.03 Å and 27.4° [23,24] and other theoretical works [25-27].

In zinc-blende bulk crystal there are two inequivalent tetrahedral interstitial positions for Mn which differ in their local environment: we denote them as Int_{As} or Int_{Ga} according whether Mn is surrounded by As or Ga atoms, respectively. There is also a hexagonal interstitial position where Mn is surrounded by *both* As and Ga atoms. In fig. 2 we show the different cases. The tetrahedral interstitial site in the ideal geometry has four

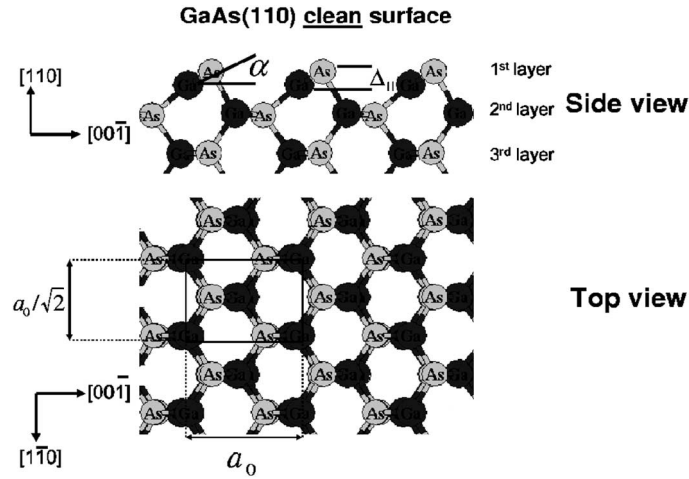**GaAs(110) <u>clean</u> surface**

Fig. 1. – Schematic side and top view of the clean GaAs(110) surface. Only the three topmost layers (1st layer is the surface layer) are shown in the figure. In this and other figures, black spheres are cations (Ga atoms), grey spheres are anions (As atoms).

nearest-neighbor (NN) atoms at a distance equal to the ideal host bond length d_1 and six next-nearest-neighbor (NNN) atoms at the distance $d_2 = \frac{2}{\sqrt{3}}d_1$, which are Ga(As) atoms for $\text{Int}_{As(Ga)}$, respectively. In the hexagonal interstitial position the Mn is surrounded by 3 As and 3 Ga atoms at distance $\sqrt{\frac{11}{12}}d_1$. Throughout this work we have considered only *tetrahedral* interstitial position (the total energy corresponding to the *hexagonal* interstitial site is higher by more than 0.5 eV) [28, 29, 8, 30].

In fig. 3 we show a ball and stick side (a) and top (b) view of the relaxed Int_{As}, Int_{Ga} configurations. Only the three topmost layers and the atoms closest to Mn are shown.
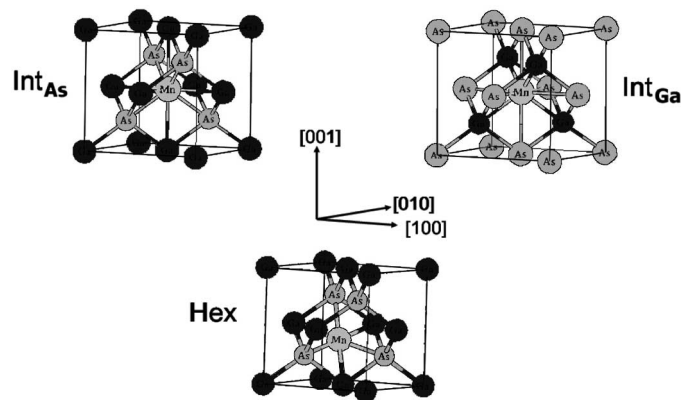

Fig. 2. – Conventional bulk unit cells representing Mn atom in tetrahedral-interstitial configurations, surrounded by As atoms (grey spheres) as nearest neighbors (top part, to the left) and by Ga atoms (black spheres) as nearest neighbors (top part, to the right). Bottom part: hexagonal interstitial position with Mn surrounded by 3 As and 3 Ga as nearest neighbors.
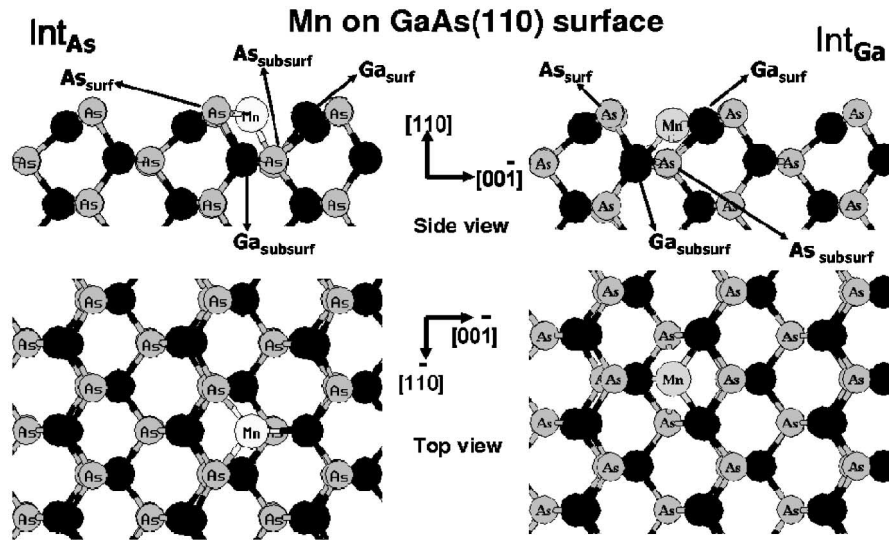
Fig. 3. – Schematic side and top view of the relaxed Int_{As} and Int_{Ga} configurations. Mn is explicitly shown.

Mn is explicitly indicated. In the relaxed structure, due to symmetry breaking because of the surface and the consequent buckling of the outermost surface layers, the NN and NNN bond lengths are no longer equal. Furthermore, some relaxed NNs bond lengths turn out to be longer than NNNs ones. In the following, we do not longer distinguish among NN and NNN (they are referred simply as NN atoms) but we simply refer to *surface* and *subsurface* atoms, as shown in the figure.

The two relaxed configurations differ in energy by ~ 130 meV/Mn atom (Int_{Ga} is favoured). This is in contrast to the bulk case, where it has been found that they differ only by ~ 5 meV/Mn [31] and Int_{As} instead is slightly favored. We have tested the reliability of our final relaxed interstitial configurations by considering different starting geometries (details in ref. [32]), other than the simple ideal (110) truncated bulk. In all cases, the final relaxed configuration is the same.

The atoms with the most sizeable displacements from the ideal zinc blende positions are the Mn impurities and their neighbors, on surface or subsurface. In table I we report the inward/outward relaxations respect to the ideal (110) surface plane.

In Int_{As}, Mn relaxes outward by ~ 0.06 Å and As_{surf} ($As_{subsurf}$) move upwards (downwards). On the other hand, the Ga atoms (both on surface and subsurface) are shifted towards the bulk.

In Int_{Ga}, Mn relaxes inward by ~ 0.32 Å; the Ga_{surf} and $Ga_{subsurf}$ atoms are displaced downwards while the As_{surf} ($As_{subsurf}$) atom moves upwards (downwards). In summary, both in Int_{Ga} and Int_{As}, cations (surface and subsurface) close to Mn move downwards, while anions upwards or downwards according whether they are on surface or subsurface. The net result is a local reduction of the surface buckling with respect to the clean unperturbed surface, more than 30% and 40% for Int_{As} and Int_{Ga}, respectively, with a net local buckling of about 0.46 Å for Int_{As} and 0.40 Å for Int_{Ga}. As far as the interatomic distances between Mn and the nearest atoms are concerned (table I), they are in general longer than the ideal bulk value by ~ 2–3%; the distances between Mn

TABLE I. – *Vertical atomic displacements with respect to ideal zinc blende bulk positions (first row) and nearest-neighbor surface and subsurface relaxed interatomic distances (second row) for Int$_{As}$ (upper part) and Int$_{Ga}$ (lower part); +/− refer to an downward/upward relaxation; the numbers in round brackets refer to unrelaxed interatomic distances. Units are in Å.*

Nearest-neighbor bond-lengths (Å)			
Int$_{As}$			
As$_{surf}$	As$_{subsurf}$	Ga$_{surf}$	Ga$_{subsurf}$
+0.15	−0.19	−0.06	−0.06
2.52(2.40)	2.44(2.40)	2.49(2.78)	2.90(2.78)
Int$_{Ga}$			
Ga$_{surf}$	Ga$_{subsurf}$	As$_{surf}$	As$_{subsurf}$
−0.22	−0.24	+0.06	−0.10
2.48(2.40)	2.56(2.40)	2.68(2.78)	2.63(2.78)

and more distant atoms are shorter than the bulk cases, except for Ga$_{subsurf}$ in Int$_{As}$, as it can be seen in table I.

3˙2. *Electronic properties*. – In fig. 4, we show the Density of States projected onto surface layer (PDOS); the continuous lines refer to Int$_{As}$ or Int$_{Ga}$ while the dashed lines refer to the clean GaAs (110) surface. DOS for Int$_{As}$(Int$_{Ga}$) are shown to the left (right) side; the Fermi level (E$_f$) is set to zero eV. The *d* Mn projected DOS is also shown (grey area). The positive and negative DOS correspond to spin-up and spin-down components. First of all, in both Int$_{As}$ and Int$_{Ga}$, the DOS curves for Int$_{As}$ and Int$_{Ga}$ are very close to those corresponding to the clean surface case, but they differ in the energy region around
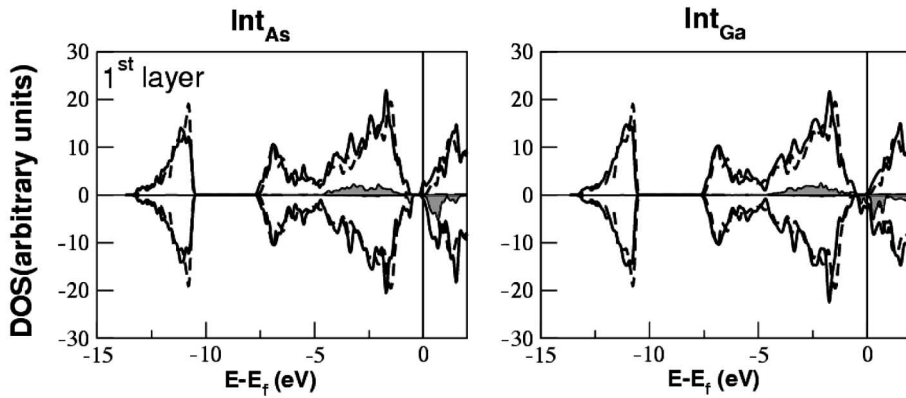

Fig. 4. – Density of States (DOS) projected into surface (continuous line) layer for Int$_{As}$ (to the left) and Int$_{Ga}$ (to the right). Dashed line corresponds to the DOS for the clean surface. Mn projected DOS is also shown (grey filled area). The Fermi level is set to zero eV.

E_f. An energy gap around E_f is present in both majority and minority DOS. In Int_{As} the majority and minority spin gaps overlap and almost coincide, maintaining the surface semiconducting with a gap of about ~ 0.2 eV. In Int_{Ga}, instead, majority and minority spin gaps are quite different: ~ 0.3 eV for the majority component and ~ 0.1 eV for the minority component. The perturbation is weak on the valence band and stronger on the conduction band. The main difference between Int_{As} and Int_{Ga} DOS curve concerns a peak in the minority component in Int_{Ga} around the Fermi energy (in Int_{As} it is shifted by 0.3–0.4 eV below the Fermi energy) which reduces the gap in Int_{Ga}.

In both systems, the Fermi level lies in the lower tail of the conduction band thus indicating that interstitial Mn impurity behaves as a donor, like in the bulk case [29].

At variance with the bulk case, where the calculated DOS for the two tetrahedral interstitial positions are almost the same [29], thus indicating a week influence of the nearest neighbors on the interstitial Mn in the two configurations, the difference between surface Int_{Ga} and Int_{As} cases is more sizeable, indicating a stronger effect of the local environment.

The PDOS almost recover the bulk features already in the second layer (not shown in fig. 4). Therefore, the introduction of Mn results in a perturbation of the electronic properties mostly localized on the first layer and strongly depending on the local environment.

As far as the d states are concerned, we observe that their contribution to the occupied majority spin component is by far larger than their contribution to the minority spin. However, their overall weight in the GaMnAs system is negligible and the valence band is in practise almost non spin-polarized (as observed above). In both cases, the Mn spin-up d states are occupied and quite similar in shape while the spin-down d states are almost unoccupied and they have a different shape, especially around the Fermi level.

In conclusion, the two Mn local environments give rise to a quite different surface electronic structure, with the differences mainly localized around the Fermi level.

3˙3. *Magnetic properties*. – In the following, we analyze the magnetic properties. The total and absolute magnetization in the supercell are different in the two configurations. They are equal to 4.23 and 4.84 μ_B in Int_{As} and to 3.41 and 4.71 μ_B in Int_{Ga}. The difference between total and absolute magnetization corresponds to the presence of region of negative spin-density in the unit cell; this difference is higher in Int_{Ga} than in Int_{As}, suggesting higher (absolute) values and/or more extended region of negative spin-density in the former than in the latter. It also justifies the smaller total magnetization of Int_{Ga} with respect to Int_{As}. This is a clear evidence that the induced magnetization is strongly influenced by the local Mn environment.

Interesting information can be gained by looking at the individual atomic magnetic moments obtained as the difference between the calculated majority and minority Lowedin charges [33]. The results have been reported elsewhere [34]. The highest value of Mn spin-polarization is found in Int_{As} (3.96 μ_B) while it is slightly lower in Int_{Ga} (3.67 μ_B). The Mn magnetic in Int_{As} is almost integer in agrement with the existence of a clear gap in the Mn-projected DOS and the unoccupied states just cutting the Fermi energy. It is worth noting that our calculated Mn magnetic moments are larger than those corresponding to the interstitial Mn in the bulk and they are rather close to the value indicated for ferromagnetically coupled substitutional Mn impurities on the Ga sublattice in bulk GaAs. In fact, *ab initio* calculations [28, 35, 36] report a Mn magnetic moment for *bulk* Int_{As} equal to 2.70 μ_B. A recent experimental work [37] show that Mn impurities on GaAs(110) surfaces have magnetic moments significantly larger compared
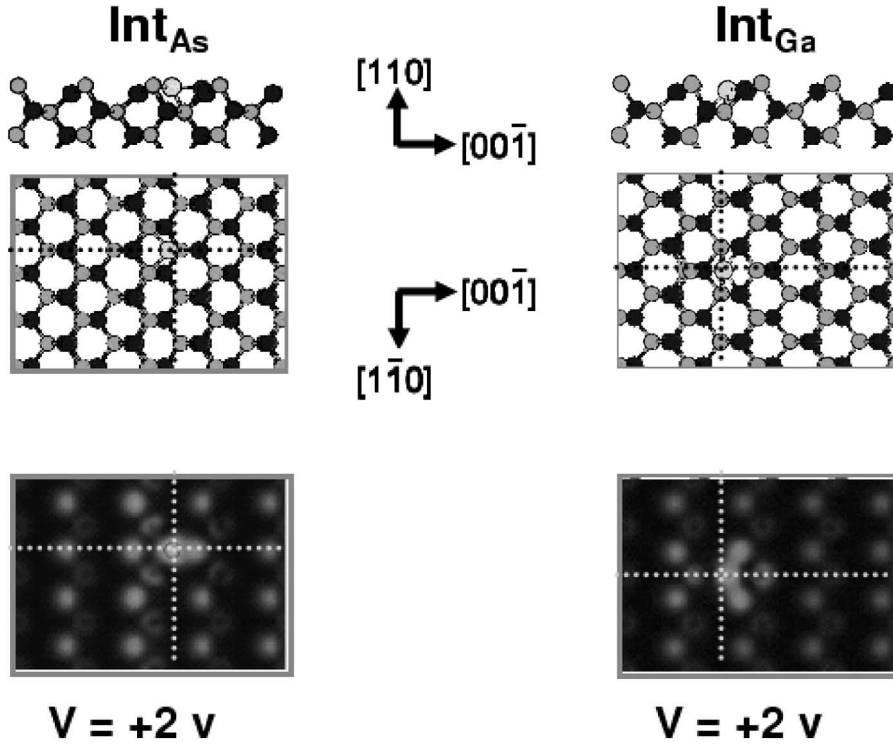
Fig. 5. – Simulated STM images of isolated Mn interstitial in GaAs(110) surface, with As NNs (to the left) and Ga NNs (to the right). Top panels: ball-and-stick model of the relaxed surface, top and side view (Ga: black spheres, As: grey spheres). Bottom panel: simulated STM images for positive bias voltage. The intersection of the dotted lines locates the position of Mn (projected on the (110) plane).

to the bulk case. The experimental and theoretical results would suggest in general an enhancement of the Mn magnetic moments due to surface effects. Our calculations, compared with previous bulk DFT studies [28, 35], support this indications.

For Int_{As}, the As_{surf} and $As_{subsurf}$ atoms have a ferromagnetic coupling to Mn, with a small magnetic moment equal to 0.05 μ_B. The induced polarization in more distant As atoms is totally negligible. The Ga_{surf} atoms couple antiferromagnetically with Mn with an induced polarization on it equal to $-0.14\mu_B$. Other atomic moments are negligible.

As far as the Int_{Ga} configuration is concerned, a negative magnetic moment is induced on Ga_{surf} $(-0.17\mu_B)$ while the $Ga_{subsurf}$ atoms have a negligible polarization. The As_{surf} shows only a negligible polarization, while it is positive and equal to 0.05 μ_B for $As_{subsurf}$.

Our results for the magnetic properties can be summarized as follows: in both cases, the cations couple antiferromagnetically to Mn spin moment while anions couple ferromagnetically. Furthermore, only surface cations are spin polarized, while both surface and subsurface anions do polarize.

4. – STM images

In fig. 5 we show the schematic top and side views of the relaxed underlying structure lattice and the XSTM images, for empty states at a reference positive bias voltages ($+2.0$ V). In Int_{Ga}, the two NN surface Ga atoms of Mn appear very bright with features extending towards the Mn and the atoms in the neighbourhood also look brighter than normal. For Int_{As}, a very bright elongated spot in the center of the surface unit cell delimited by As is visible. We would like to point out that the simulated XSTM images have clearly different shape for the two geometric configurations, so the two different local coordinations should be distinguished by STM analysis. Further, the simulated STM images for Int_{As} case well compare with experimental XSTM images of the δ-doped samples [11].

5. – Conclusion

In summary, we have used first-principles simulations to characterize Mn interstitial impurity on the GaAs (110) surface. Strong local distortion on the (110) GaAs surface are introduced by Mn, especially when it is surrounded by Ga atoms. In both case, Mn polarizes the NN and NNN atoms, giving rise to a ferromagnetic Mn–As and to an antiferromagnetic Mn–Ga configuration. The simulated STM images show very different shape of the imaged Mn atom, suggesting that two configurations can be clearly differentiated by STM analysis. Finally, recent experimental STM images are qualitatively similar to our simulated one for Int_{As} configuration, suggesting the possible identification of Mn interstitials surrounded by As atoms in the experimental samples [11].

$$* * *$$

REFERENCES

[1] Sharma P., *Science*, **307** (2005) 531.
[2] Covington M., *Science*, **307** (2005) 215.
[3] Ohno Y., Young D. K., Beschoten B., Matsukura F., Ohno H. and Awschalom D. D., *Nature*, **402** (1999) 790.
[4] Ohno H., Matsukura F. and Ohno Y., *Mater. Sci. Eng. B*, **84** (2001) 70.
[5] Yu K. M., Walukiewicz W., Wojtowicz T., Kuryliszyn I., Liu X., Sasaki Y. and Furdyna J. K., *Phys. Rev. B*, **65** (2002) 201303.
[6] Bergqvist L., Korzhavyi P. A., Sanyal B., Mirbt S., Abrikosov I. A., Nordström L., Smirnova E. A., Mohn P., Svedlindh P. and Eriksson O., *Phys. Rev. B*, **67** (2003) 205201.
[7] Edmonds K. W., Wang K. Y., Campion R. P., Neumann A. C., Farley N. R. S., Gallagher B. L. and Foxon C. T., *Appl. Phys. Lett.*, **81** (2002) 4991.

[8] EDMONDS K. W., BOGUSLAWSKI P., WANG K. Y., CAMPION R. P., NOVIKOV S. N.,
     FARLEY N. R. S., GALLAGHER B. L., FOXON C. T., SAWICKI M., DIETL T., NARDELLI
     M. B. and BERNHOLC J., *Phys. Rev. Lett.*, **92** (2004) 37201.
[9] NAZMUL A. M., SUGAHARA S. and TANAKA M., *Phys. Rev. B*, **67** (2003) R241308.
[10] NAZMUL A. M., AMEMIYA T., SHUTO Y., SUGAHARA S. and TANAKA M., *Phys. Rev.
     Lett.*, **95** (2005) 017201.
[11] MODESTI S. and FURLANETTO D., personal communication.
[12] MIKKELSEN A., SANYAL B., SADOWSKI J., OUATTARA L., KANSKI J., MIRBT S.,
     ERIKSSON O. and LUNDGREN E., *Phys. Rev. B*, **70** (2004) 85411.
[13] SULLIVAN J. M., BOISHIN G. I., WHITMAN L. J., HANBICKI A. T., JONKER B. T. and
     ERWIN S. C., *Phys. Rev. B*, **68** (2003) 235324.
[14] YAKUNIN A. M., SILOV A. Y., KOENRAAD P. M., WOLTER J. H., VAN ROY W., DE
     BOECK J., TANG J. M., FLATTÉ M. E., *Phys. Rev. Lett.*, **92** (2004) 216806.
[15] YAKUNIN A. M., SILOV A.Y., KOENRAAD P. M., TANG J.-M, FLATTÉ M. E., VAN ROY
     W., DE BOECK J. and WOLTER J. H., cond-mat/0505536 preprint (2005).
[16] BARONI S., DAL CORSO A., DE GIRONCOLI S., GIANNOZZI P. and CAVAZZONI C.,
     `http://www.pwscf.org`.
[17] CEPERLY D. M. and ADLER B. J., *Phys. Rev. Lett.*, **45** (1980) 566.
[18] PERDEW J. and ZUNGER A., *Phys. Rev. B*, **23** (1981) 5048.
[19] VANDERBILT D. H., *Phys. Rev. B*, **41** (1990) 7892.
[20] For the optimation of atomic positions we require Hellmann-Feynman forces smaller than
     0.02 eVÅ^{-1}.
[21] OW KING N. and WANG X. W., *Phys. Rev. B* **54** (1996) 17661.
[22] TERSOFF J. and HAMANN D., *Phys. Rev. B*, **31** (1985) 805.
[23] EBERT P., *Surf. Sci. Rep.*, **33** (1999) 121.
[24] FORD W. K., GUO T., LESSOR D. L. and DUKE C. B., *Phys. Rev. B*, **42** (1990) 8952.
[25] MIOTTO R., SRIVASTAVA G. P. and FERRAZ A. C., *Phys. Rev. B*, **59** (1999) 3008.
[26] FERRAZ A. C. and SRIVASTAVA G. P., *Surf. Sci.*, **182** (1987) 161.
[27] UMERSKI A. and SRIVASTAVA G. P., *Phys. Rev. B* , **51** (1995) 2334.
[28] MÁCA F. and MAŠEK J., *Phys. Rev. B*, **65** (2002) 235209.
[29] MAŠEK J. and MÁCA F., *Phys. Rev. B*, **69** (2004) 165212.
[30] CAO J. X., GONG X. G. and WU R. Q., *Phys. Rev. B*, **72** (2005) 153410.
[31] MAŠEK J., KUDRNOVSKÝ J. and MÁCA F., *Phys. Rev. B*, **67** (2003) 153203.
[32] STROPPA A. and PERESSI M., *Mater. Sci. Eng. B*, **126** (2006) 217.
[33] LOEWDIN P. O., *J. Chem. Phys.*, **18** (1950) 365.
[34] STROPPA A. and PERESSI M., in preparation.
[35] SANYAL B. and MIRBT S., *J. Magn. Magn. Mater.*, **290-291** (2005) 1408.
[36] WU R., *Phys. Rev. Lett.*, **94** (2005) 207201.
[37] GAMBARDELLA P., BRUNE H., DHESI S. S., BENCOK O., KRISHNAKUMAR S. R.,
     GARDONIO S., VERONESE M., GRAZIOLI C. and CARBONE C., *Phys. Rev. B*, **72** (2005)
     45337.
[38] KOKALJ A., *Comp. Mater. Sci.*, **28** (2003) 155. Code available from `http://www.`
     `xcrysden.org/`.